Molecular Biology of the Cell
Vol. 19, 237–247, January 2008

Expansion of the Nucleoplasmic Reticulum Requires the Coordinated Activity of Lamins and CTP:Phosphocholine Cytidylyltransferase α

Karsten Gehrig,* Rosemary B. Cornell,† and Neale D. Ridgway*

*Departments of Pediatrics, and Biochemistry and Molecular Biology, Atlantic Research Centre, Dalhousie University, Halifax, NS, Canada B3H 4H7; and †Department of Molecular Biology and Biochemistry, Simon Fraser University, Burnaby, BC, Canada V5A 1S6

Submitted February 27, 2007; Revised October 1, 2007; Accepted October 17, 2007
Monitoring Editor: Jennifer Lippincott-Schwartz

The nucleoplasmic reticulum (NR), a nuclear membrane network implicated in signaling and transport, is formed by the biosynthetic and membrane curvature-inducing properties of the rate-limiting enzyme in phosphatidylcholine synthesis, CTP:phosphocholine cytidylyltransferase (CCT) α. The NR is formed by invagination of the nuclear envelope and has an underlying lamina that may contribute to membrane tubule formation or stability. In this study we investigated the role of lamins A and B in NR formation in response to expression and activation of endogenous and fluorescent protein-tagged CCTα. Similarly to endogenous CCTα, CCT-green fluorescent protein (GFP) reversibly translocated to nuclear tubules projecting from the NE in response to oleate, a lipid promoter of CCT membrane binding. Coexpression and RNA interference experiments revealed that both CCTα and lamin A and B were necessary for NR proliferation. Expression of CCT-GFP mutants with compromised membrane-binding affinity produced fewer nuclear tubules, indicating that the membrane-binding function of CCTα promotes the expansion of the NR. Proliferation of atypical bundles of nuclear membrane tubules by a CCTα mutant that constitutively associated with membranes revealed that expansion of the double-bilayer NR requires the coordinated assembly of an underlying lamin scaffold and induction of membrane curvature by CCTα.

INTRODUCTION

The nuclear envelope (NE) is composed of an outer membrane contiguous with the endoplasmic reticulum (ER) and an inner membrane with an underlying nuclear matrix or lamina. The two membranes are separated by a luminal space but are joined at nuclear pores interspersed throughout the NE and by protein bridging assemblies that interact with the nuclear lamina and the cytoplasmic cytoskeleton (Gruenbaum *et al.*, 2005). The NE exhibits discrete tissue-specific changes in size, shape, and morphology (i.e., nuclear folds, invaginations, and lobes) during development (Brandt *et al.*, 2006), the cell cycle (Prunuske and Ullman, 2006), and aging (Goldman *et al.*, 2004; Haithcock *et al.*, 2005). These morphological changes are dependent on A- and B-type nuclear lamins, type-V intermediate filament proteins, that multimerize and provide structural support but are also involved with a variety of other functions including apoptosis, nuclear envelope assembly, and DNA replication and transcription (Prunuske and Ullman, 2006). Mutations in lamin A and associated proteins result in altered nuclear shape and size and influence chromatin organization, DNA repair, and structural integrity, resulting in heritable human disorders such as progeria (Eriksson *et al.*, 2003), muscular dystrophy (Bonne *et al.*, 1999), and lipodystrophy syndromes (Shackleton *et al.*, 2000). Although it is evident that the nuclear lamina controls nuclear morphology, it is unknown how this is coordinated with the synthesis of nuclear membranes that are also required for shape and size changes. In this regard, we recently showed that the nuclear rate-limiting enzyme for phosphatidylcholine (PtdCho) synthesis, CTP:phosphocholine cytidylyltransferase (CCT) α, in addition to regulating bulk phospholipid synthesis, is specifically involved in expansion of an intranuclear membrane network termed the nucleoplasmic reticulum (NR; Lagace and Ridgway, 2005). The NR is a complex membrane network that contains integral membrane and luminal proteins derived from the ER, nuclear pore complex, and cytosolic components within the core of tubules (Fricker *et al.*, 1997; Johnson *et al.*, 2003b). By extending the NE into the nucleus, the NR expands the nuclear/cytoplasmic interface, potentially increasing transport and communication between these compartments and providing structural support to the nucleus. On a functional level, the NR is a site for IP_3-gated calcium release and signaling in the nuclear interior (Lui *et al.*, 1998; Echevarria *et al.*, 2003; Marius *et al.*, 2006). The observed interaction of CCTα with the NR provides the first evidence that changes in nuclear morphology is directly linked to membrane synthesis and remodeling.

This article was published online ahead of print in *MBC in Press* (http://www.molbiolcell.org/cgi/doi/10.1091/mbc.E07–02–0179) on October 24, 2007.

Address correspondence to: Neale D. Ridgway (nridgway@dal.ca).

Abbreviations used: CCT, CTP:phosphocholine cytidylyltransferase; CPT, choline phosphotransferase; ConA, concanavalin A; DAG, diacylglycerol; DsRed, *discosoma* red fluorescent protein; DiOC6, 3,3′-dihexyloxacarbocyanine iodide; GFP, green fluorescent protein, NE, nuclear envelope; NPC, nuclear pore complex; NR, nucleoplasmic reticulum; PtdCho, phosphatidylcholine; RNAi, RNA interference; siRNA, short interfering RNA.

Supplemental Material can be found at:
http://www.molbiolcell.org/content/suppl/2007/10/23/E07-02-0179.DC1.html

CCTα is ubiquitously expressed in mammalian tissues and contains a N-terminal nuclear localization signal (NLS) that mediates nuclear import in many but not all cells (Wang *et al.*, 1993b, 1995; Ridsdale *et al.*, 2001; Fagone *et al.*, 2007). The structurally related CCTβ1 and β2 isoforms are encoded by a separate gene, expressed at variable levels in human tissues and localized to the cytoplasm and ER (Lykidis *et al.*, 1998, 1999). CCTα contains a 50-amino acid amphipathic α-helix termed domain M that embeds into membranes enriched in negatively charged lipids such as fatty acids and phosphatidylglycerol or nonbilayer forming lipids such as phosphatidylethanolamine and diacylglycerol (DAG; Attard *et al.*, 2000; Davies *et al.*, 2001). Addition of exogenous fatty acids (Wang *et al.*, 1993a; Lagace *et al.*, 2000) or elevated DAG levels (Watkins and Kent, 1992) promotes CCTα translocation to the inner NE, dissociating domain M from the catalytic domain and decreasing the K_m for CTP (Cornell and Northwood, 2000). Thus CCTα domain M senses the composition of membranes with regard to the content of PtdCho precursors (fatty acids and DAG) and/or PtdCho content and makes appropriate adjustments in catalytic activity and metabolic flux through the CDP-choline pathway.

CCTα activation at the NE is required for bulk PtdCho synthesis, but it also specifically regulates invagination of the NE to form the NR. Previous data suggested that CCTα-dependent NR proliferation proceeds by two mechanisms: increased synthesis of PtdCho and/or formation of tubules by inducing positive curvature of existing membranes (Lagace and Ridgway, 2005). Because association of domain M with membranes is intimately linked to enzyme activation and PtdCho synthesis, these two mechanisms are not mutually exclusive but rather coordinate NR tubule formation. However, the observed increase in NR tubule formation by a constitutively active mutant lacking domain M (CCTΔ236) that does not associate with membranes suggests that additional factors can drive NR formation if sufficient phospholipids are available. On the other hand, catalytically dead CCTα mutants were as effective as the wild-type in inducing NR proliferation, showing that CCTα can induce nuclear tubule formation without increasing PC synthesis, via a direct effect of domain M on membrane morphology (Lagace and Ridgway, 2005). CCTα homodimers have a combined domain M hydrophobic surface area estimated to be 2000 A^2 (Dunne *et al.*, 1996) that if inserted into a lipid bilayer would significantly affect lipid packing. At a ratio as low as 2 CCTα dimers per vesicle, CCTα dimers cross-bridge and aggregate vesicles composed of PtdCho and phosphatidylglycerol (Taneva *et al.*, 2005). When the concentration of CCTα was increased (>1500 CCT/vesicle) mixed phospholipid vesicles containing 5 mol% oleate were deformed into 50-nm tubules by increasing positive curvature of the outer leaflet due to insertion of domain M. This type of surface property, predicted by the "bilayer couple hypothesis" (Sheetz *et al.*, 1976), occurs when a surface area incongruity is caused by insertion of a protein into one leaflet of the bilayer, resulting in net membrane curvature (Ford *et al.*, 2002; Farsad and De Camilli, 2003; Lee *et al.*, 2005).

Although membrane synthesis and induction of positive membrane curvature by CCTα can drive NR formation, it is probable that other components of the NR are required to stabilize and extend membrane tubules. Microscopy of the NR has revealed an underlying proteinaceous laminar matrix similar to the NE (Fricker *et al.*, 1997; Lagace and Ridgway, 2005). The frequency of lamin A–positive NR tubules also increased in CHOK1 cells treated with oleate, indicating that a lamin scaffold underlies the expanding NR network (Lagace and Ridgway, 2005). Here we used RNA interference (RNAi) and a temperature-sensitive cell line to show that CCTα and lamins A and B1 are required for NR proliferation. Overexpression studies using fluorescent-tagged CCTα and lamins A and B1 revealed that coexpression was required to elicit massive expansion of the NR. Proliferation of abnormal stacks of membrane tubules caused by expression of a CCTα mutant that constitutively associated with membranes indicated that ordered expansion of the double-bilayered NR requires the coordinated polymerization of an underlying lamin network.

MATERIALS AND METHODS

Materials

An oleate/bovine serum albumin (BSA) complex (6.8:1, mol/mol) was prepared by converting oleic acid (Matreya, State College, PA) dissolved in ethanol (10 mM) to the sodium salt by addition of NaOH. The salt was dried under N_2 and dissolved in 150 mM NaCl and 10% BSA (wt/vol) by stirring at 20°C. This oleate/BSA ratio gives an estimated free oleate concentration of ~1 μM (Richieri *et al.*, 1993). A polyclonal antibody against lamin B1 (sc-6216) was from Santa Cruz Biotechnology (Santa Cruz, CA). The monoclonal lamin A/C antibody used for immunofluorescence was from Santa Cruz Biotechnology (sc-7293), whereas a polyclonal used for immunoblotting was from Cell Signaling Technologies (Beverly, MA). The green fluorescent protein (GFP) mAb, 3,3′-dihexyloxacarbocyanine iodide (DiOC6), AlexaFluor-conjugated secondary antibodies, AlexaFluor-conjugated concanavalin A (ConA), and Lipofectamine 2000 were from Invitrogen (Carlsbad, CA). The CCTα antibody was directed against the C-terminal phosphorylation domain (Yang *et al.*, 1997). EDTA-free protease inhibitor cocktail tablets were from Roche Diagnostics (Mannheim, Germany). siRNA duplexes for lamin A (GAACUGCAGCAUCAUGUAAUU), A/C (GUACGGCUCUCAUCAACUCUU), and B1 (ACACAUCAGUCAGUUACAAUU) were supplied by Dharmacon (Lafayette, CO). The siRNA transfection reagent TransIT-TKO was from Mirus (Madison, MI).

Plasmids

ptetGFP vectors expressing lamin A/C and B1 fused at the N-terminal with GFP (ptetGFP-WTLMB1 and pEGFPhLA-WT) were provided by Dr. David Gilbert (SUNY Upstate Medical University, NY). pCCT-GFP and a monomeric version of pCCT-*discosoma* red fluorescent protein (DsRed, Clontech, Palo Alto, CA) were constructed by subcloning the HindIII/SacII fragment from pcDNA-CCT-V5/His (Lagace and Ridgway, 2005) into pEGFP-N1 and pDsRED-N1, respectively. CCT and CCT-3EQ were also fused to a monomeric version of GFP (L221K; Snapp *et al.*, 2003; Zacharias *et al.*, 2002) to confirm that GFP multimerization did not affect localization. cDNAs encoding CCT-5KQ (K248,252,259,266Q,R245Q), CCT-8KQ (K248,250, 252,254,259,261, 266Q; R245Q), and CCT-3EQ (E257,268,279Q; Johnson *et al.*, 2003a) were digested with EcoRV and BspHI, and the fragments encoding the mutant domain M were subcloned into pcDNA-CCT-/V5-His. The resulting pcDNA-CCT-V5/His constructs were then digested with HindIII and SacII, and the CCTα cDNAs were ligated into pEGFP-N1 or pDsRed-N1.

Cell Culture and Transfections

Chinese hamster ovary (CHO) cells were cultured in an atmosphere of 5% CO_2 in DMEM, 5% fetal calf serum (FCS), and 34 μg/ml proline at 37°C. CHO MT58 (CHO58) cells were maintained under the same conditions but at 33°C. CHOK1 and CHO58 cells cultured on glass coverslips or glass-bottom dishes were transiently transfected at 37°C with vectors encoding fluorescent protein-tagged CCTα or lamins for 12–18 h using Lipofectamine 2000. CHO58 cells were then transferred to 40°C for 1 h followed by addition of serum-free Ham's F12 medium with 10 mM HEPES (pH 7.4) for 1 h before stimulation with oleate/BSA. CHOK1 cells were treated the same but were maintained at 37°C. For live cell imaging, CHO58 cells were switched to serum-free F12 medium containing 10 mM HEPES (pH 7.4) and 0.2% BSA, and transferred to the heated stage (40°C) of a Nikon EclipseT2000-E inverted microscope (Melville, NY) equipped with a 60× oil immersion lens (1.6 NA) and GFP filter set.

Short interfering RNA (siRNA) duplexes for lamin A, A/C, B1 or nontargeting (NT) controls (50 nM each) were transfected into CHOK1 cells using Trans-IT-TKO transfection reagent for 48 h.

Enzyme Assays

CCT activity in extracts from CHO58 cells transiently transfected with CCT-GFP or CCT-DsRed was assayed as previously described (Cornell and Vance, 1987). Cells were harvested in cold PBS, sedimented at 2000 × *g* for 5 min, and homogenized in 20 mM Tris-HCl (pH 7.4), 1 mM dithiothreitol, 1 mM EDTA, and protease inhibitor cocktail by 10 passages through a 23-gauge needle. Homogenates were subject to centrifugation (10,000 × *g* for 10 min), and the

supernatant was assayed for conversion of [^{14}C]phosphocholine to [^{14}C]CDP-choline at 37°C for 20 min in the presence and absence of 1 mM PtdCho/oleic acid (1:1, mol/mol) vesicles or variable ratios as indicated in the legend to Figure 6.

PtdCho synthesis was measured by [^{3}H]choline incorporation into PtdCho in transiently transfected CHO58 at 40°C. Cells were pulse-labeled with [^{3}H]choline for 1 h in the presence or absence of 300 μM oleate/BSA in choline-deficient DMEM, 5% lipoprotein-deficient serum, and 34 μg/ml proline. [^{3}H]PtdCho was extracted from cells and quantified by liquid scintillation counting (Storey *et al.*, 1997).

Fluorescence Microscopy

After plasmid or siRNA transfection, cells were treated with or without oleate/BSA in Ham's F12 medium for the times indicated in figure legends, fixed in 4% paraformaldehyde, permeabilized with 0.05% Triton X-100, and incubated with primary antibodies against lamin A/C, lamin B1, CCTα, and/or Alexafluor-conjugated ConA, followed by an appropriate Alexafluor-conjugated secondary antibody (Lagace and Ridgway, 2005). Cellular membranes were visualized by incubating live cells with 0.25 μg/ml DiOC6 in Ham's F12 medium for 10 min at 40°C. Coverslips were viewed using a Zeiss LSM 510 Meta/Axiovert 100M inverted microscope (Thornwood, NY) with a 100× (1.4 NA) oil immersion objective. Three-dimensional images were reconstructed from 15 to 21 consecutive 0.2–0.5-μm sections using the Zeiss LSM Image Viewer.

Three-dimensional reconstructions of cells stained with Alexafluor-conjugated ConA were used to identify and quantify NR tubules as previously described (Lagace and Ridgway, 2005). Briefly, filamentous structures staining with ConA continuous with the nuclear envelope and spanning ≥50% of the nucleus were identified as NR tubules. Data sets generated from reconstructed multiple optical sections through the nucleus were similar to results with single optical sections (0.5 μm) through the midnuclear region of cells that stained for ConA.

Thin-Section and Immunoelectron Microscopy

Transfected CHO58 cells were fixed for 2 h at room temperature with 4% paraformaldehyde plus 0.5% glutaraldehyde in 0.1 M sodium cacodylate buffer, pH 7.2. Cell pellets postfixed in 2% (wt/vol) osmium tetroxide in cacodylate buffer were embedded, sectioned, and poststained with 2% (wt/vol) uranyl acetate and lead citrate. Ultrathin sections (80–100 nm) were viewed using a Philips EM300 electron microscope (Mahwah, NJ; Lagace and Ridgway, 2005). For immunoelectron microscopy (immuno-EM), cells were fixed, sectioned, and mounted on 200-mesh nickel grids as previously described (Lagace and Ridgway, 2005). Grids were incubated with an anti-GFP mAb for 1 h followed by an affinity-purified goat anti-rabbit IgG conjugated to 5-nm colloidal gold for 2 h. Controls consisted of samples processed with no primary antibody. Before viewing, grids were fixed with 2.5% glutaraldehyde and stained with 2% (wt/vol) uranyl acetate/lead citrate.

RESULTS

Association of Fluorescent Protein-tagged CCTα with the NR

Immunofluorescence studies in fixed cells showed that CCTα overexpression induced the formation of nuclear tubules containing lamin A and ConA-reactive ER/NE glycoproteins (Lagace and Ridgway, 2005). To study the dynamics and coordination of CCTα and lamins in the NR expansion process, we used GFP-tagged lamin A and B1 (Izumi *et al.*, 2000) and constructed and functionally characterized C-terminal CCTα-GFP and monomeric DsRed fusion proteins. We opted to attach GFP to the C-terminus of CCTα because an N-terminal tagged GFP-CCT, though catalytically active and nuclear-localized, appeared to have impaired translocation to the NE (DeLong *et al.*, 2000). Fusion proteins were expressed in CHO58 cells, which have 80–90% of wild-type CCTα expression at 37°C and virtually undetectable activity at the nonpermissive temperature of 40–42°C (Esko *et al.*, 1981; Lagace and Ridgway, 2005). Transient expression of CCT-GFP or CCT-DsRed in CHO58 cells at 40°C yielded the expected 65–70 kDa fusion proteins (Figure 1A) and was accompanied by an increase in CCT activity measured in cell lysates in vitro (Figure 1B). This activity was stimulated 5- to 10-fold by PtdCho/oleate vesicles, showing that GFP- and DsRed-tagged CCT mimic untagged CCT in its response to anionic vesicles (Feldman *et al.*, 1985; Figure 1B). Expression of CCT-GFP also restored PtdCho synthesis in intact CHO58 cells at 40°C (Figure 1C). In living CHO58 cells cultured at 40°C, CCT-GFP was uniformly localized in the nucleoplasm with no evidence of cytoplasmic fluorescence (Figure 1D). Complete membrane translocation of endogenous CCTα is reliably induced by delivery of oleate from a BSA carrier (Cornell and Vance, 1987; Wang *et al.*, 1993a; Lagace and Ridgway, 2005). Similarly, exposure of CHO58 cells to 300 μM oleate/BSA at 40°C resulted in translocation of nucleoplasmic CCT-GFP to punctate nuclear structures after 15–20 min (the Quicktime movie from which these frames were taken is shown in Supplementary Figure 1). The dissociation of CCT-GFP from the nuclear structures was assessed by replacing oleate-

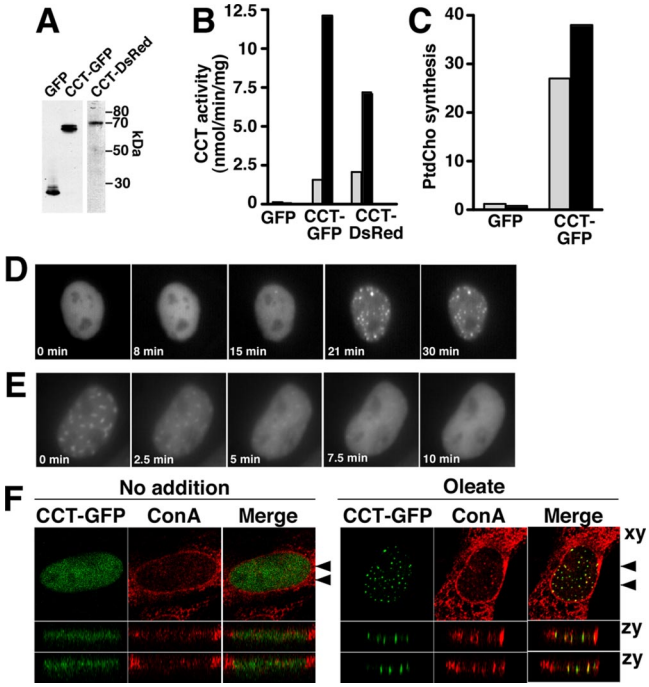

Figure 1. CCT-GFP reversibly translocates to NR tubules. (A) GFP, CCT-GFP, or CCT-DsRed were transiently overexpressed in CHO58 cells for 14 h at 33°C before switching to 40°C for 1 h. Total cell lysates (20 μg) were separated by SDS-10%PAGE and immunoblotted using a GFP (CCT-GFP and GFP lanes) or CCTα (CCT-DsRed lane) polyclonal antibody. (B) CCT activity in soluble fractions isolated from CHO58 cells expressing GFP, CCT-GFP, or CCT-DsRed were assayed in the absence (▨) or presence (■) of 1 mM PtdCho/oleate (1:1, mol/mol) vesicles. Results are the mean of duplicates from a representative experiment. (C) [^{3}H]Choline incorporation into PtdCho (DPM/μg cell protein) was quantified in CHO58 cells transiently expressing GFP or CCT-GFP at 40°C. Cells were pulse-labeled in the absence (▨) or presence (■) of 300 μM oleate/BSA for 1 h. Results are the mean of duplicates from a representative experiment. (D) CHO58 cells transiently expressing CCT-GFP at 40°C were exposed to 300 μM oleate/BSA. Images were captured (150–200-ms exposures) at 30-s intervals for up to 30 min using a Photometrics Cascade 512B CCD camera (Woburn, MA) and Metamorph software program (Universal Imaging, West Chester, PA). (E) CHO58 cells were stimulated with oleate/BSA for 20 min as described in D. Medium was then replaced with prewarmed (40°C) oleate-free F12 medium with 0.2% BSA, and images were captured at 30-s intervals. (F) CHO58 cells expressing CCT-GFP were treated with oleate or no addition for 15 min, fixed, and stained with AlexaFluor647-conjugated ConA. Confocal sections (0.2 μm) in the xy plane (top panels) were reconstructed to give two cross-sectional views (indicated by arrows) of the zy plane (lower panels).

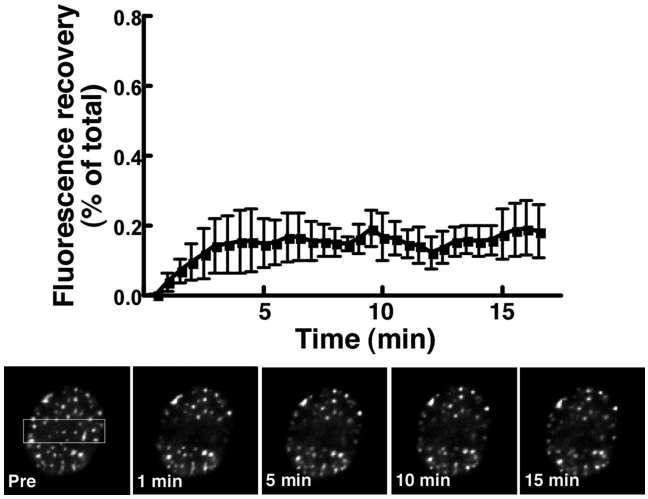

Figure 2. CCT-GFP associates stably with the NR. CHO58 cells expressing CCT-GFP were treated with oleate/BSA for 20 min as described in the legend to Figure 1D. Photobleaching experiments were performed using Nikon EclipseT2000-E inverted microscope equipped with a 100× oil immersion lens and Nikon Eclipse-D C1 confocal with a 488-nm argon laser. Selected areas of nuclei were photobleached (indicated by the boxed area in the prebleach cell) with the 488-nm laser at full power, and images were captured at 30-s intervals (150–200-ms exposures) for 15–20 min. Fluorescence recovery was calculated using the ratio of fluorescence in the bleached nuclear region/total cell fluorescence at each time point divided by the initial prebleach ratio. Results are the mean and SD of three experiments that examined a total of 12 nuclei each.

containing media after 20 min with media containing 0.2% BSA. This resulted in rapid and complete dissociation of CCT-GFP from intranuclear structures and dispersion into the nucleoplasm by 5 min (Figure 1E). In fixed oleate-treated CHO58 cells, CCT-GFP colocalized with numerous ConA-positive tubules that vertically transverse the nucleus when viewed in the zy plane (Figure 1F). CCT-GFP was also localized to the nuclear envelope in 60.8% of oleate-treated CHO cells (n = 118) that contained abundant NR localization (Supplementary Figure 2A). We also determined if GFP dimerization affected CCT localization by determining the localization of CCT fused to monomeric GFP L122K (mGFP; Zacharias *et al.*, 2002; Snapp *et al.*, 2003). CCT-mGFP was nucleoplasmic and translocated to the NR in response to oleate (Supplementary Figure 2B). Similar to CCT-GFP, CCT-mGFP was active in vitro and promoted proliferation of ConA-positive NR tubules (results not shown).

Fluorescent recovery after photobleaching (FRAP) was used to assess the stability of CCT-GFP interaction with the NR (Figure 2). CCT-GFP was translocated to the NR in oleate-treated CHO58 cells and fluorescent recovery was measured in photobleached regions comprising about a third of the nucleus. Only 21.1 ± 8.7% of CCT-GFP was in the mobile fraction (Lippincott-Schwartz *et al.*, 2001) at 17 min, suggesting stable interaction with the NR in the presence of oleate. Thus CCT-GFP functionally mimics endogenous CCTα and stably interacts with the NR in the presence of a lipid activator.

Lamin A or B1 Association with the NR Is Dependent on CCTα

CCTα- and/or oleate-induced NR formation was detected by increased lamin A/C colocalization with CCTα in the nuclear tubules (Lagace and Ridgway, 2005). To demonstrate that the presence of the lamins in the NR was linked to increased CCTα expression, we probed for lamin staining of intranuclear tubules in cells with or without CCTα. CHOK1- and CCTα-temperature labile CHO58 cells were cultured at 40°C for 1 h and treated with 350 μM oleate/BSA for 20 min, and localization of ConA, lamin A/C, and lamin B1 was visualized by immunostaining and confocal micros-

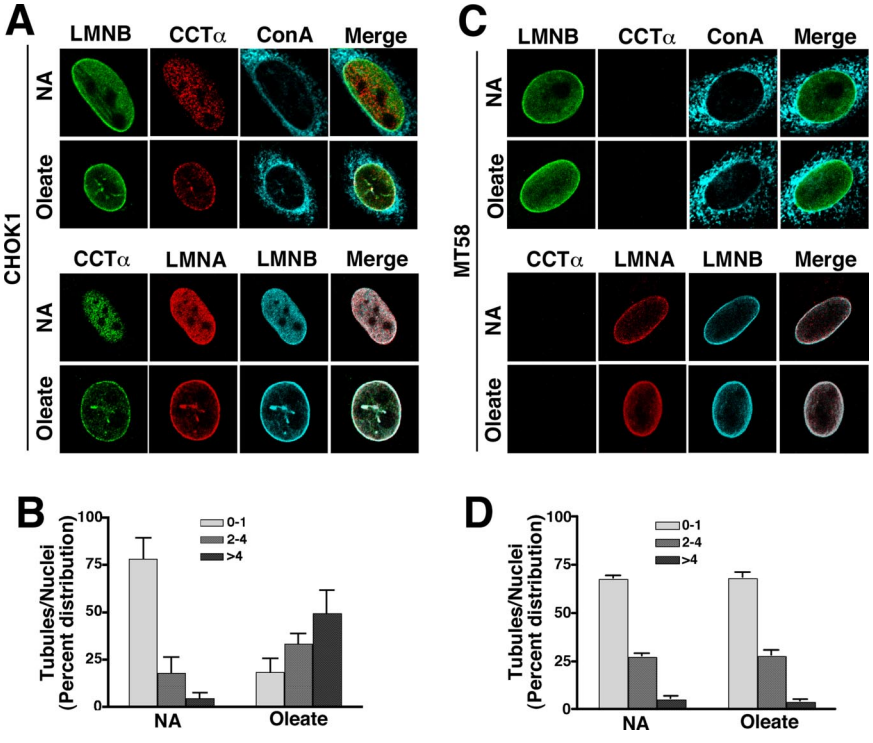

Figure 3. Formation of a lamin-enriched nucleoplasmic reticulum requires CCTα. (A) CHOK1 cells cultured in DMEM with 5% delipidated FCS received no addition (NA) or 350 μM oleate/BSA for 20 min before fixing and permeabilization with Triton X-100. CCTα was localized with a primary polyclonal antibody and AlexaFluor594- (top panel) or AlexaFluor488-conjugated (bottom panel) secondary antibodies. Lamin B1 was localized with primary and AlexaFluor488 (top panel) or AlexaFluor647 (bottom panel) secondary antibodies. Lamin A/C was visualized with a monoclonal primary antibody and AlexaFluor594 secondary antibody (bottom panel). ER, NE, and NR membranes were visualized with AlexaFluor647-ConA (top panel). (B). The percent distribution of ConA-positive NR tubules/nuclei was quantified in cells treated with oleate or no addition (NA). Results are the mean and SD of 40 nuclei from three separate experiments. (C) CHO58 cells cultured at 40°C were treated with and without oleate and immunostained as described in A. (D) The percent distribution of ConA-positive NR tubules/nuclei was quantified in CHO58 cells. Results are the mean and SD of 40 nuclei from three separate experiments. LMNA, lamin A; LMNB, lamin B1.

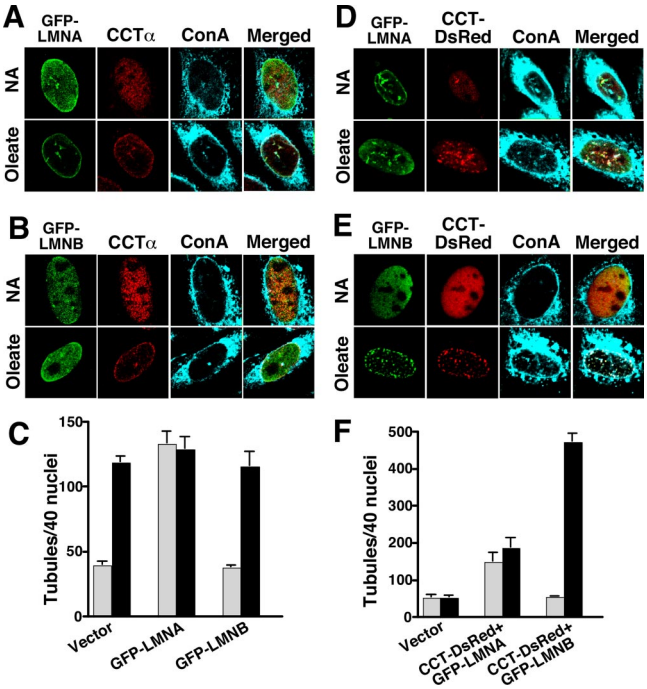

Figure 4. Lamin A and B1 expression promotes NR proliferation. (A and B) CHOK1 cells were transiently transfected with GFP-lamin A (A) or GFP-lamin B1 (B). Cells then received no addition (NA) or 350 μM oleate/BSA for 20 min at 37°C and were fixed and incubated with AlexaFluor647-ConA. Endogenous CCTα was detected with a primary polyclonal and AlexaFluor594-conjugated secondary antibodies. (C) ConA-positive tubules were quantified in 40 nuclei of control (▨) or oleate-treated (■) cells from three separate experiments. (D and E) CHO58 cells were double-transfected with GFP-lamin A and CCT-DsRed (D) or GFP-Lamin B1 and CCT-DsRed (E) at 37°C, treated with oleate or no addition at 40°C, and incubated with AlexaFluor647-ConA as described above. (F) ConA-positive tubules were quantified in 40 nuclei of control (▨) or oleate-treated (■) cells from three separate experiments.

copy (Figure 3). Untreated CHOK1 cells expressed abundant nuclear CCTα, lamin A/C and B distributed to the NE or diffusely throughout the nucleoplasm (Figure 3A). Treatment of CHOK1 cells with oleate resulted in the appearance of numerous intranuclear filaments corresponding to the NR that costained for lamin A/C, lamin B1, CCTα, and ConA. Quantitation of the NR showed that oleate treatment of CHOK1 cells caused a dramatic shift in the proportion of cells containing 2–4 and >4 tubules/nuclei (Figure 3B). CCTα expression was undetectable in CHO58 cells cultured at the nonpermissive temperature in the absence of oleate, but lamin A/C and lamin B1 were distributed in the nucleoplasm and NE similar to CHOK1 cells (Figure 3C). Unlike CHOK1 cells, oleate addition to CHO58 cells did not result in increased lamin A/C, lamin B1, or ConA localization to NR tubules. The distribution of NR tubules in control and oleate-treated CHO58 cells was virtually identical to the majority of cells (70%) containing 0–1 tubule/nuclei (Figure 3D). These experiments suggest that endogenous lamin A/C and B1 associate with the NR in a CCTα-dependent manner.

Expression of Lamin A or B Is Required for Proliferation of the NR

Because the expression of endogenous lamins was not sufficient to generate a NR network in the absence of CCTα, it appeared that the initiating event was membrane synthesis/deformation or that coordination with lamin assembly was required. To further explore this relationship, we tested whether overexpression of lamins, in the context of endogenous CCTα or overexpressed CCTα, was sufficient to promote NR proliferation. For these experiments, GFP-lamin A or GFP-lamin B1 was expressed individually in CHOK1 cells or coexpressed with CCT-DsRed in CCT-deficient CHO58 cells and ConA-positive NR tubules were quantified (Figure 4). Baseline NR tubule formation (quantified by ConA staining) was established in control and oleate-treated CHOK1 and CHO58 cells transfected with pGFP or pDsRed (distribution shown in Figure 4, C and F, and Supplementary Figure 3). NR tubules were increased in CHOK1 cells expressing GFP-lamin A in the presence and absence of oleate but CCTα colocalized with GFP-lamin A only in fatty acid–treated cells (Figure 4A). GFP-lamin B1 did not increase NR tubule formation either in control or oleate-treated cells (Figure 4B). Quantification of results from Figure 4, A and B, showed that CHOK1 cells expressing GFP-lamin A displayed a significant increase in ConA-positive NR tubules in the absence of oleate and no change upon fatty acid addition (Figure 4C). CHOK1 cells transfected with GFP-lamin B1 had baseline and oleate-stimulated NR tubule distribution that was similar to vector controls (Figure 4C). In contrast to results for individual expression of GFP-lamin A and B1, coexpression of GFP-lamins and CCT-DsRed in CHO58 cells had a substantially greater effect on NR proliferation (Fig-

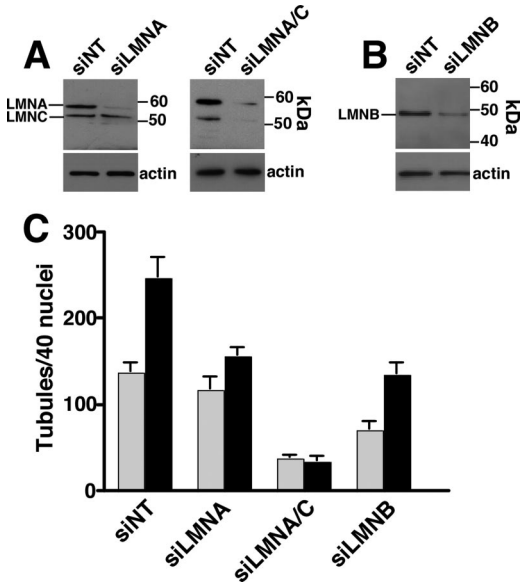

Figure 5. Lamin A/C and B depletion by RNAi prevents NR tubule proliferation. (A) CHOK1 cells were transiently transfected with a nontargeting siRNA (NT) or siRNAs specific for lamin A of lamin A/C. After 48 h, total cell lysates were prepared and immunoblotted with a lamin A/C antibody. Filters were also probed for actin to demonstrate similar protein loading. (B) CHOK1 cells were transfected with an siNT or a lamin B1-specific siRNA, and total cell lysates immunoblotted with a lamin B1-specific antibody. (B) After transient transfection for 48 h with nontargetting, lamin A, or lamin B1 siRNAs, cells were treated with or without 350 μM oleate/BSA in serum-free DMEM for 30 min, fixed and incubated with AlexaFlour488-ConA, and immunostained for lamin A/C and lamin B1. The frequency of NR tubules based on Alexafluor488-ConA staining was quantified in 40 nuclei from untreated (▨) or oleate-treated (■) cells. Results are the mean and SD of three separate experiments. Abbreviations: LMNA, lamin A; LMNA/C, lamin A/C; LMNB, lamin B1.

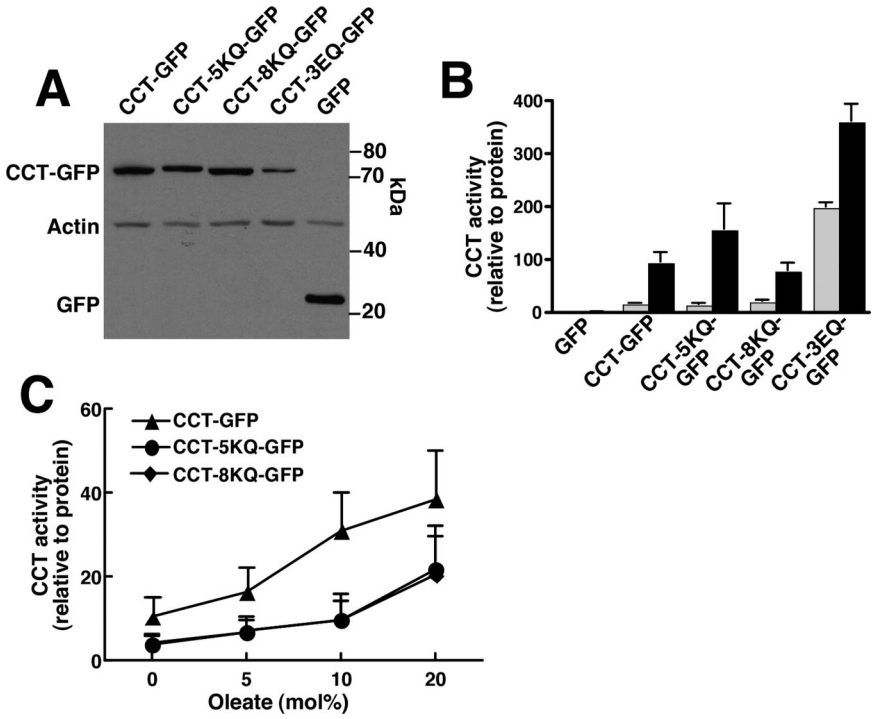

Figure 6. Enzyme activity of GFP-CCTα domain M mutants. (A) Domain M mutants of CCTα and empty vector (GFP) were transiently transfected into CHO58 cells at 37°C for 12 h. Cells were then transferred to 40°C for 30 min, and total cell lysates were prepared and immunoblotted for CCT-GFP fusion proteins with an anti-GFP antibody. Blots were also probed with actin to demonstrate equal protein load. (B) CHO58 cell lysates were assayed for CCT activity in the absence (▨) or presence (■) of 1 mM PtdCho/oleate (1:1, mol/mol) vesicles. Activity was normalized to expression of GFP or CCT-GFP proteins as determined by densitometry. Results are the mean and SD of three separate experiments. (C) Activity of wild type, CCT-5KQ, and CCT-8KQ was assayed using PtdCho vesicles with increasing mol% oleate as described in B. Results are the mean and SD of three experiments.

ures 4, D–F). Coexpression of GFP-lamin A with CCT-DsRed increased NR tubule formation in the absence and presence of oleate, and there was evidence of CCT-dsRed association with the NR in unstimulated cells (Figure 4D). More dramatic results were observed in CHO58 cells coexpressing GFP-lamin B1 and CCT-dsRed (Figure 4E). Oleate treatment completely shifted the distribution of both CCT-dsRed and GFP-lamin B1 from a diffuse nucleoplasmic distribution to numerous punctate structures that colocalized with ConA. Quantification of NR distribution showed that coexpression of GFP-lamin A and CCT-dsRed increased tubules in the presence and absence of oleate (Figure 4F). Coexpression of GFP-lamin B1 and CCT-dsRed increased oleate-dependent tubule formation 10-fold compared with mock-transfected controls. The effect of lamin and CCT expression on the distribution of NR tubules in cell nuclei is shown in Supplementary Figure 3. Compared with cells expressing GFP or DsRed, lamin A expression, either alone or in combination with CCT, shifted the distribution in favor of nuclei with multiple tubules in the presence or absence of oleate. Coexpression of GFP-lamin B1 and CCT-DsRed in oleate-treated CHO58 cells caused a striking shift to >95% nuclei with four or more NR tubules.

To further test this relationship, lamin A/C and lamin B1 expression was suppressed with siRNA, and resulting effects on NR tubule formation were quantified (Figure 5). Compared with CHOK1 cells transfected with a nontargeting siRNA, transfection of siRNAs directed against lamin A

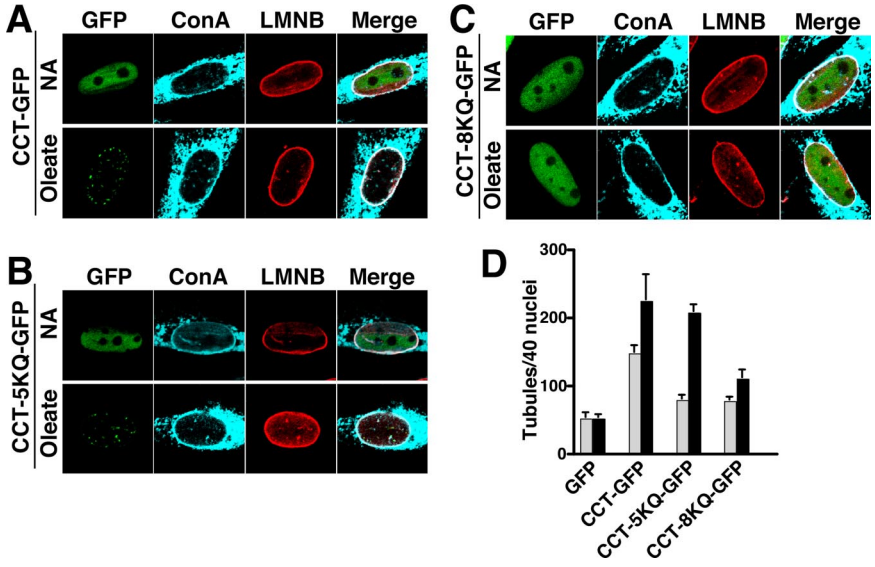

Figure 7. CCTα domain M mutants with reduced membrane affinity do not promote NR proliferation. CHO58 cells transiently expressing (A) CCT-GFP, (B) CCT-5KQ-GFP, or (C) CCT-8KQ-GFP were transferred to 40°C for 1 h and then treated with no addition (NA) or 300 μM oleate/BSA for 15 min. Cells were processed for immunofluorescence and incubated with AlexaFluor647-ConA and with a lamin B1 primary and AlexaFluor594 secondary antibody. (D) In each case, NR tubule frequency was quantified based on AlexaFluor647-ConA staining of control (▨) or oleate-treated (■) cells. Results are the mean and SD of three experiments.

(Figure 5A), lamin A plus the lamin C splice variant (Figure 5A), or lamin B1 (Figure 5B) reduced expression of target proteins by 70–90%. CHOK1 cells transfected with nontargeting (NT) siRNA displayed the expected increase in NR tubule formation in response to oleate as quantified by staining with ConA (Figure 5C). Knockdown of lamin A had no effect on baseline NR tubules but suppressed the oleate-mediated increase in NR proliferation (Figure 5C). Knockdown of both lamin A and C expression reduced basal NR tubules by 75% and completely abrogated the effect of oleate. In contrast, depletion of lamin B1 reduced NR tubules by 50% in the absence of oleate but did not prevent a approximately twofold increase in the number of tubules by oleate treatment. Representative immunofluorescence images of CHOK1 cells transfected with lamin A, lamin A/C, and lamin B1 siRNAs and treated with oleate are shown in Supplementary Figure 4. Although previous studies have shown that knockout or knockdown of lamin A and B expression alters nuclear morphology and increases cell death (Harborth *et al.*, 2001; Lammerding *et al.*, 2006), RNAi of lamin A/C and B1 in CHO cells did not appear to affect nuclear structure (Supplementary Figure 4) or increase apoptosis (measured by a nucleosome release assay, results not shown). This series of experiments (Figures 3–5) show that formation of tubular invaginations of the NE requires the coordinated activity of CCTα for membrane synthesis/remodeling and formation of an underlying lamin network.

The Membrane-binding Function of CCTα Is Required for Proliferation of the NR

RNAi and overexpression studies indicated a coordinated assembly of NR tubules involving CCTα and nuclear lamins but did not differentiate between membrane remodeling/synthesis or lamina reorganization as the initiating event. To gain further insight into the mechanism of NR formation, we examined the effect of several CCTα mutants with increased or decreased membrane binding on proliferation of the NR. Replacement of five or eight lysine or arginine residues with glutamine (CCT-5KQ and CCT-8KQ, respectively) in a domain M peptide resulted in reduced binding to anionic lipid vesicles (Johnson *et al.*, 2003a). Analysis of these mutants should allow us to determine if domain M is the primary driving force behind NR proliferation or whether other factors are required. GFP-fusions of CCT-5KQ and 8KQ were constructed and transiently expressed into CHO58 cells at the nonpermissive temperature. The mutants were expressed as intact fusion proteins and at comparable levels to CCT-GFP in whole cell lysates (Figure 6A). Soluble cell extracts were assayed for CCT activity in the presence and absence of PtdCho/oleate (1:1, mol/mol) vesicles, a concentration of fatty acid that provides maximal activation, and normalized to expression of the individual GFP-fusion proteins (Figure 6B). CCT-GFP, CCT-5KQ-GFP, and CCT-8KQ-GFP had similar basal activity that was stimulated five- to eightfold by PtdCho vesicles containing 50 mol% oleate (Figure 6B). However, when assayed with vesicles composed of 5–20 mol% oleate, 5KQ and 8KQ mutants displayed reduced activation relative to wild type, indicating compromised membrane binding (Figure 6C).

Next, the capacity of CCT-5KQ and -8KQ to induce NR tubule formation was measured by transient expression in CHO58 cells and oleate treatment for 15 min (Figure 7A). After oleate treatment, CCT-GFP and CCT-5KQ-GFP translocated to nuclear punctate structures that costained with ConA and lamin B1 (Figures 7, A and B). CCT-8KQ-GFP displayed incomplete oleate-dependent translocation to the

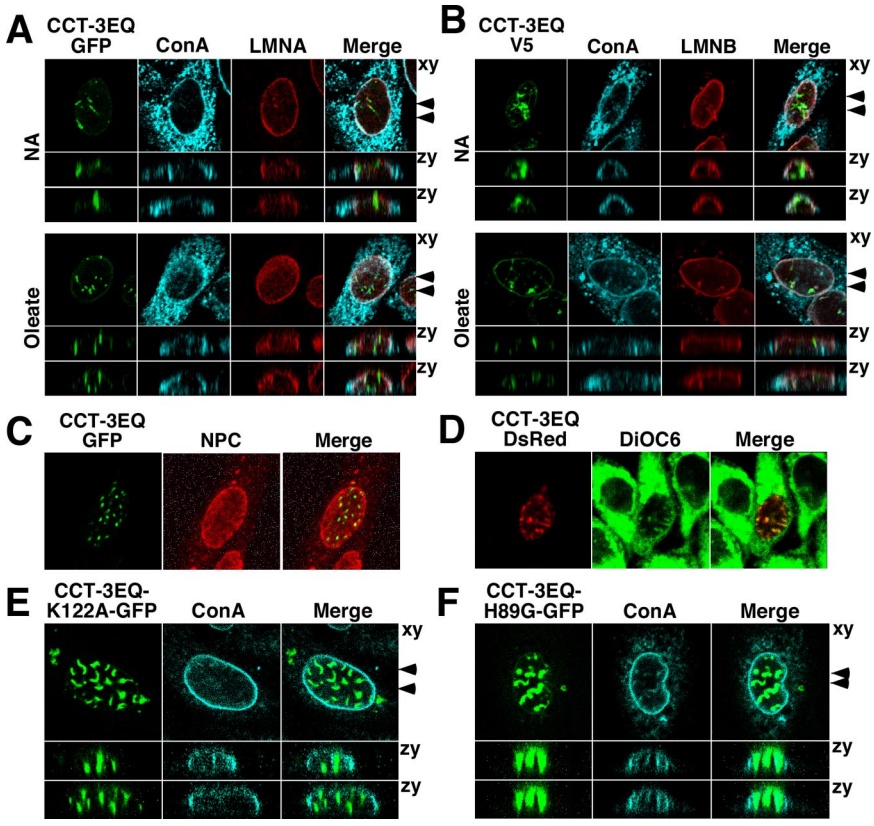

Figure 8. Constitutively active, membrane-associated CCT-3EQ promotes nuclear membrane proliferation. (A) CHO58 cells were transiently transfected with CCT-3EQ-GFP at 37°C, transferred to serum-free conditions at 40°C for 1 h, and then treated with addition (NA) or 300 μM oleate/BSA for 15 min at 40°C. Cells were processed for immunofluorescence, incubated with AlexaFluor647-ConA, and immunostained with lamin A/C primary and AlexaFluor594 secondary antibodies. A single 0.5-μm confocal section in the xy plane is shown. Serial confocal sections (15 sections of 0.5 μm each) were used to reconstruct the two images in the zy plane (arrows in xy plane indicate the positions). (B) CHO58 cells were transiently transfected with pcDNA-CCT-3EQ-V5/His and treated as described in A. Fixed cells were incubated with AlexaFluor647-ConA and immunostained with V5 and lamin B1 primary and AlexaFluor-488 or -594 secondary antibodies, respectively. (C) CHO58 cells transiently expressing CCT-3EQ-GFP were fixed and immunostained with nuclear pore complex (NPC)-specific antibody against Nup62 and an AlexaFluor-594 secondary antibody. (D) CHO58 cells transiently expressing CCT-3EQ-DsRed were incubated with DiOC6 to visualize total cellular membranes. (E and F) CHO58 cells were transiently transfected with catalytically dead CCT-3EQ/H89G-GFP or CCT-3EQ/K122A-GFP, treated with 300 μM oleate/BSA for 15 min, stained with AlexaFluor674-ConA, and viewed by serial confocal sections as described in A.

NR; ~70% of cells displayed partial or absent NE or NR translocation, and these had no evidence of lamin B1 or ConA-positive tubules (Figure 7C). Quantification of immunofluorescence images for GFP (vector) and CCT-GFP–transfected cells revealed that CCT-GFP increased the basal and oleate stimulated formation of NR tubules compared with vector-transfected controls (Figure 7D). CCT-8KQ-GFP expressing cells had significantly diminished tubule formation in the presence and absence of oleate but levels were still increased relative to vector controls. The 5KQ mutant had an intermediate phenotype; the number of NR tubules under basal conditions was diminished but oleate activation was similar to CCT-GFP. These results suggest that a primary determinant of nuclear tubule production is the membrane affinity of domain M in CCTα.

Constitutively Membrane-associated and -activated CCTα Promotes Abnormal Nuclear Membrane Proliferation

Substitution of three glutamates with glutamine (CCT-3EQ) increased domain M hydrophobicity and membrane affinity, while reducing selectivity for anionic lipids (Johnson *et al.*, 2003a). In transfected CHO58 cells, CCT-3EQ-GFP was expressed at a slightly lower level than wild-type or the lysine/arginine mutants (Figure 6A), but its in vitro activity in cell extracts was increased eightfold above controls under basal conditions and was enhanced an additional twofold by PtdCho/oleate vesicles (Figure 6B). These activity measurements reflect the constitutive membrane association of CCT-3EQ-GFP.

When expressed in CHO58 cells, CCT-3EQ-GFP was observed in large irregular intranuclear structures that did not colocalize with ConA or lamin A/C (Figure 8A). CCT-3EQ association with these structures was independent of oleate treatment, consistent with its constitutive membrane association. Reconstruction of serial confocal sections through a nucleus viewed in the zy plane indicated that CCT-3EQ-GFP–positive structures were orientated vertically and in close proximity to the NE under control and oleate-treated conditions. V5-tagged CCT-3EQ transiently expressed in CHO58 cells also localized to similar large intranuclear structures in the presence and absence of oleate (Figure 8B). CCT-3EQ-V5 positive structures were irregularly shaped and relatively devoid of lamin B1 and ConA fluorescence. NPC is also present in NR tubules (Fricker *et al.*, 1997; Lagace and Ridgway, 2005), but in this case the NPC subunit Nup62 displayed minimal overlap with CCT-3EQ-GFP (Figure 8C). Although structures containing CCT-3EQ did not contain constituents of the NR, positive staining with the lipophilic dye DiOC6 indicated the presence of abundant membrane lipids (Figure 8D). To determine whether these membrane structures were formed as a result of the catalytic or membrane curvature–inducing activity of CCTα, the localization of catalytically dead versions of CCT-3EQ-GFP (H89G and K122A; Veitch *et al.*, 1998; Helmink *et al.*, 2003; Lagace and Ridgway, 2005) was examined in CHO58 cells (Figure 8, E and F). CCT-3EQ/K122A-GFP (Figure 8E) and CCT-3EQ/H89G-GFP (Figure 8F) were concentrated in nuclear structures in oleate-treated CHO58 cells that were similar to the catalytically active CCT-3EQ (both mutants were concentrated in similar structures in untreated cells, result not shown). Similar to CCT-3EQ-GFP, these structures had minimal overlap with ConA-positive membrane glycoproteins. This indicates that domain M, and not ongoing PtdCho synthesis, is sufficient to promote the proliferation of these unusual nuclear membrane structures.

The ultrastructure of nuclei from CHO58 cells expressing CCT-3EQ-GFP was examined in more detail by negative staining and thin-section EM (Figure 9). Micrographs of nuclei expressing CCT-GFP showed cross sections of double membrane tubules with an underlying lamina that was indistinguishable from NR tubules from CHO cells expressing endogenous or epitope-tagged CCTα (Lagace and Ridgway, 2005; Figure 9, A–D). Oleate treatment caused the appearance of more nuclei containing multiple tubule cross sections (indicated by arrows in Figure 9C). Transient expression of CCT-3EQ-GFP in CHO58 cells produced a variety of large membranous structures in control and oleate-treated cells (Figure 9, E–L): These consisted primarily of membrane stacks (panels F and J) that when sectioned at right angles revealed the presence of densely packed circular structures (panels H and J). Higher magnification of a membrane stack (Figure 9, M and N) showed ordered layers of membranes that at points of cross section revealed narrow tubular openings. These tubules did not have an electron dense lamina and were not composed of a double bilayer, and individual tubules had a diameter of 20–25 nm compared with 100–500 nm for the NR. The possibility that these tubules were the result of GFP dimerization was discounted because expres-

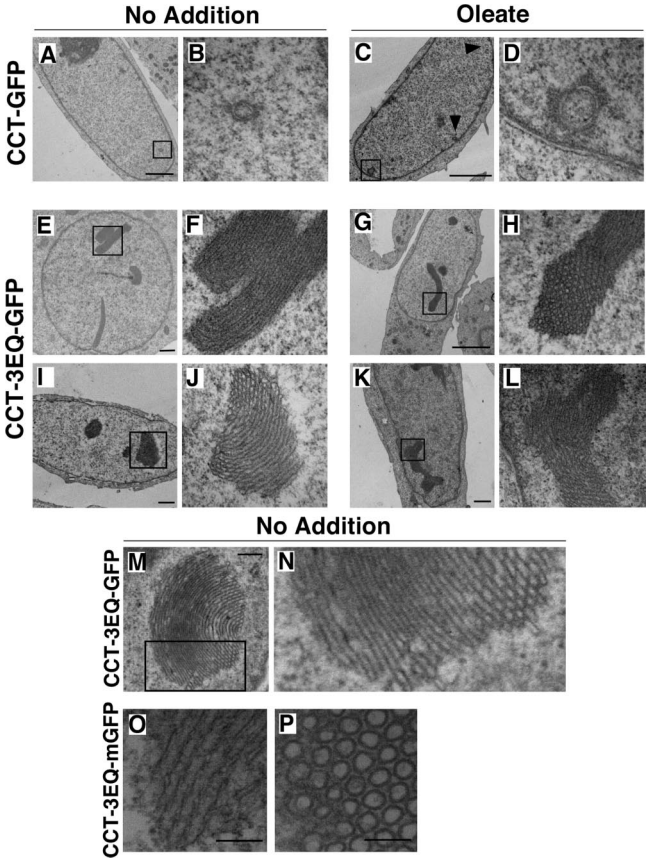

Figure 9. CCT-3EQ causes formation of intranuclear stacks of membrane tubules. CHO58 cells were transfected with CCT-GFP or CCT-3EQ-GFP at 37°C, switched to 40°C for 1 h, and treated without (NA) or with 300 μM oleate/BSA for 15 min. Cells were then fixed, embedded, and sectioned for EM analysis. Low-magnification fields are shown in A, C, E, G, I, and K (bar, 2 μm), and corresponding selected high-magnification fields are shown in B, D, F, H, J, and L. (M) A large membrane stack in a CCT-3EQ-GFP–expressing cell (bar, 500 nm). (N) Magnification of selected field from M. (O and P) Longitudinal and cross section of tubule bundles from nuclei of CCT-3EQ-mGFP–expressing cells (bar, 100 nm).

sion of CCT-3EQ-mGFP produced identical structures (Figure 9, O and P).

To determine how CCT-3EQ-GFP associated with these tubular membrane stacks, immuno-EM was preformed in CHO58 cells transiently expressing wild type and CCT-3EQ-GFP (Figure 10). CCT-GFP was diffusely localized in the nucleus (Figure 10, A and B) and upon oleate treatment concentrated around faint circular structures (indicated by arrows in panel B) that appeared to be NR tubules. Control or oleate-treated CHO58 cells expressing CCT-3EQ-GFP contained abundant immunogold particles that colocalized with stacks of membrane tubules (Figure 10, C and D). High magnification of one of these (areas in E are enlarged in F and G) indicated CCT-3EQ was distributed uniformly throughout the stacks of membrane tubules that are shown in cross section (indicated by arrows in F) and longitudinal section (indicated by arrows in G). In addition, the membrane tubule stack shown in panel E appeared to be in close contact with the NE.

DISCUSSION

The NE forms a boundary for communication and transport between the nucleus and cytoplasm. The interface between these two compartments can be expanded by dynamic invaginations of NE to form a reticular network termed the NR. Our biochemical, cytological, and ultrastructure studies indicate that NR proliferation requires that membrane proliferation and deformation mediated by the rate-limiting enzyme in PtdCho synthesis is coordinated with assembly of a supporting lamin scaffold.

To expand on previous fixed cell studies, the dynamics of CCT translocation in living cells was characterized using a GFP-fusion protein. Oleate stimulated CCT-GFP catalytic activity in vitro, and in living CHO cells promoted rapid and reversible translocation to the NR tubules based on a vertical orientation that transversed the nuclei and colocalization with ConA and lamins. Similar to CCTα overexpression, transient expression of CCT-GFP resulted in increased ConA-positive NR tubules in the absence or presence of oleate (Figure 7D). This suggests that although CCT-GFP may translocate to existing tubules, it also drives the formation of the NR. Activation of CCT-GFP appeared to favor NR localization; however, 60% of NR-positive cells also displayed localization to the NE. This localization pattern was not due to the fluorescent tags because monomeric versions of GFP and DsRed gave similar results. Rather, this apparent shift in distribution to the NR is likely a consequence of acute activation of CCT.

Induction of the NR Is Sensitive to the Ratios of Lamin B1 and CCTα Present in the Nucleus

The colocalization of endogenous lamin A/C and B with ConA-positive NR tubules was dependent on oleate activation of CCTα (Figure 3). However, overexpression of lamin A and B1 had differing effects on NR proliferation. Similar to previous reports (Broers *et al.*, 1999; Izumi *et al.*, 2000), overexpression of GFP-lamin A resulted in increased formation of nuclear filaments that was independent of activation of endogenous CCTα with oleate (Figure 4A). Similarly, cotransfection of GFP-lamin A and CCT-GFP resulted in oleate-independent NR tubule formation. These results suggested that lamin A can induce NR without an increase in CCTα-membrane association and activation and that CCTα and lamin A do not specifically cooperate to enhance NR proliferation. However, siRNA knockdown experiments in CHO cells revealed that lamin A expression was required for oleate-stimulated NR proliferation and that depletion of both lamin A/C markedly suppressed basal NR. Thus a specific threshold of lamin A/C expression is necessary for CCTα-mediated NR proliferation. In contrast, GFP-lamin B1 had no effect on the NR when expressed alone but in combination with CCT-DsRed promoted a 10-fold increase in oleate-stimulated tubule formation (relative to vector control) without affecting basal levels. This, together with a 50% reduction of both basal and oleate-stimulated NR proliferation in cells depleted of lamin B1, indicates that NR assembly is sensitive to CCTα and lamin B1 stoichiometry.

The different roles for lamin A/C and B1 in NR assembly and proliferation is likely due to the C-terminal CaaX farnesylation motif. The C-type lamin is a splice variant missing the CaaX motif, whereas A-type lamins are farnesylated but the group is removed by proteolytic processing in the nucleus (Lin and Worman, 1993; Young *et al.*, 2006). The farnesyl group on B-type lamins is permanently attached (reviewed in Gruenbaum *et al.*, 2005) and would incorporation into the membranes of an extending NR tubule. This could serve to stabilize the tubule by initiating the formation of a

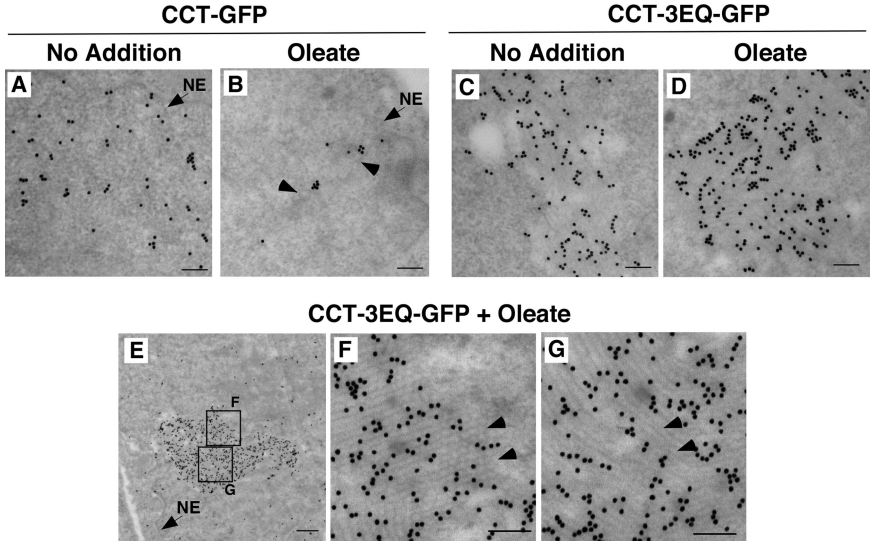

Figure 10. CCT-3EQ-GFP is interspersed in membrane tubule stacks. CHO58 cells were transfected with CCT-GFP or CCT-3EQ-GFP and treated with or without oleate as described in the legend to Figure 9. Ultra-thin sections of fixed cells were analyzed by immuno-EM using an anti-GFP polyclonal and goat anti-rabbit secondary conjugated to 5-nm colloidal gold. (A–D) Representative fields from control and oleate-treated cells (bars, 100 nm). Arrows in B indicate NR-like structures. Location of NE is indicated in A and B. (E) Low-magnification of a membrane stack from an oleate-treated CCT-3EQ-GFP–transfected CHO58 cell nuclei (bar, 500 nm). Location of NE is indicated. (F and G) Two selected high-magnification fields from E (bar, 100 nm). Arrows indicate regions of cross section (F) and lengthwise section (G) of membrane stacks.

lamin scaffold or further enhance positive membrane curvature by insertion of the farnesyl group into the nucleoplasmic leaflet of the NR (Prufert *et al.*, 2004; Ralle *et al.*, 2004).

The Membrane-binding Strength of CCT Influences NR Expansion

Mutation of domain M interfacial lysine residues (CCT-5KQ and CCT-8KQ) reduced affinity for anionic membranes based on peptide binding assays (Johnson *et al.*, 2003a). When expressed in the context of the full-length protein, both mutants had wild-type activity in the presence of 50 mol% oleate but were poorly activated between 5 and 20 mol% oleate. In intact cells, this translated into partially compromised CCT-5KQ activity with respect to promoting NR proliferation under basal conditions, whereas the 8KQ mutant had reduced ability to form NR tubules under both basal and oleate-stimulated conditions. This supports the idea that the membrane-binding strength of domain M of CCTα controls the extent of NR expansion. The substitution of a weak membrane binding CCT such as CCT-8KQ for wild-type CCT likely has two consequences with regard to nuclear tubule enhancement: reduced curvature induction and reduced PC synthesis rates.

The effect of enhancing domain M binding on the NR was illustrated by mutations of key glutamic acid residues (CCT-3EQ) that negated the requirement for protonation at the interface of anionic membranes as a prelude to binding (Johnson *et al.*, 2003a). CCT-3EQ-GFP was highly active in the absence of oleate and promoted the proliferation of intranuclear bundles of membrane tubules that were distinct from the NR. These tubules were deficient in ConA-positive glycoproteins, lamins A/C and B1, and NPCs and were single-bilayer, suggesting they derived from invaginations of the inner NE. Thus the resulting imbalance between membrane abundance/deformation and the supply of lamins and associated proteins linking the inner and outer NE would result in proliferation of single bilayer tubules derived from the inner NE.

Enhanced CCT–Membrane Interaction Is Sufficient to Induce Nuclear Membrane Expansion

Membrane deforming proteins have been identified that induce positive curvature and membrane tubulation in vitro and in vivo (Farsad *et al.*, 2001; Yoon *et al.*, 2001; Lee *et al.*, 2002, 2005). However, CCTα is the first protein to induce such structures in the nucleus. Proliferation of the inner NE occurs when nuclear proteins (Isaac *et al.*, 2001; Sorensen *et al.*, 2004) and lamins (Prufert *et al.*, 2004; Ralle *et al.*, 2004) are overexpressed, but these are membrane whorls or lamellar structures formed by low-affinity protein–protein interactions (Snapp *et al.*, 2003; Sorensen *et al.*, 2004). In contrast, CCT-3EQ induced bundles of narrow diameter membrane tubules (20–25 nm, Figure 10) that were smaller than the NR (100–500 nm) but similar to those formed in vitro by recombinant CCTα binding to vesicles (20–50 nm; Lagace and Ridgway, 2005). Because CCTα is dimeric (Cornell, 1989), formation of tubule bundles could be the result of CCTα dimers, forming domain M cross-bridges between adjacent tubules (Taneva *et al.*, 2005).

Nuclear membrane proliferation by CCT-3EQ could also result from enhanced catalytic activity augmenting the supply of the limiting metabolite in PtdCho synthesis, CDP-choline. This seems unlikely since expression of catalytically dead versions of CCT-3EQ produced an abundance of similar structures (Figure 8, E and F). This, together with our previous observation of increased NR tubule formation in response to oleate activation of catalytically dead wild-type CCTα (Lagace and Ridgway, 2005), indicates that the curvature-inducing activity of domain M is sufficient to drive membrane tubulation in the nucleus. However, under conditions where membrane components are not limiting, NR tubule extension could be promoted by other factors. Indeed, lamin A expression was sufficient to increase NR tubules independent of CCTα activation indicating that other membrane deforming functions operate within the laminar matrix.

The collective results of these studies indicate that stoichiometric expression of nuclear lamins, particularly the B-type, and CCTα are required for NR invaginations of the NE. Disrupting the balance in favor of CCTα hyperactivation and limiting lamin expression resulted in atypical bundles of single-bilayer tubules. This indicates that lamins have a potentially important role in NR formation by linking the inner and outer NE, perhaps via UNC-84-UNC83 or UNC-84-nesprin interactions (Gruenbaum *et al.*, 2005). Validation of these and other lamin and CCTα interactions will provide future insight into the assembly, structure, and function of the NR.

ACKNOWLEDGMENTS

Robert Zwicker provided technical assistance in tissue culture. Gary Faulkner and Mary-Ann Trevors assisted in EM analysis. Advice and assistance with live cell imaging and FRAP analysis was provided by Xiaohui Zha (Ottawa Health Research Institute, Ottawa, ON). CCT-5KQ, 8KQ, and 3EQ mutants were constructed by Mingtang Xie (Simon Fraser University, Burnaby, BC). This research was supported by Canadian Institutes of Health Research Operating Grants 62916 (to N.D.R) and 12134 (to R.B.C). K.M.G is the recipient of an Issac Walton Killiam Graduate Studentship.

REFERENCES

Attard, G. S., Templer, R. H., Smith, W. S., Hunt, A. N., and Jackowski, S. (2000). Modulation of CTP:phosphocholine cytidylyltransferase by membrane curvature elastic stress. Proc. Natl. Acad. Sci. USA *97*, 9032–9036.

Bonne, G. *et al.* (1999). Mutations in the gene encoding lamin A/C cause autosomal dominant Emery-Dreifuss muscular dystrophy. Nat. Genet. *21*, 285–288.

Brandt, A. *et al.* (2006). Developmental control of nuclear size and shape by Kugelkern and Kurzkern. Curr. Biol. *16*, 543–552.

Broers, J. L., Machiels, B. M., van Eys, G. J., Kuijpers, H. J., Manders, E. M., van Driel, R., and Ramaekers, F. C. (1999). Dynamics of the nuclear lamina as monitored by GFP-tagged A-type lamins. J. Cell Sci. *112*(Pt 20), 3463–3475.

Cornell, R. (1989). Chemical cross-linking reveals a dimeric structure for CTP:phosphocholine cytidylyltransferase. J. Biol. Chem. *264*, 9077–9082.

Cornell, R., and Vance, D. E. (1987). Translocation of CTP:phosphocholine cytidylyltransferase from cytosol to membranes in HeLa cells: stimulation by fatty acid, fatty alcohol, mono- and diacylglycerol. Biochim. Biophys. Acta *919*, 26–36.

Cornell, R. B., and Northwood, I. C. (2000). Regulation of CTP:phosphocholine cytidylyltransferase by amphitropism and relocalization. Trends Biochem. Sci. *25*, 441–447.

Davies, S. M., Epand, R. M., Kraayenhof, R., and Cornell, R. B. (2001). Regulation of CTP:phosphocholine cytidylyltransferase activity by the physical properties of lipid membranes: an important role for stored curvature strain energy. Biochemistry *40*, 10522–10531.

DeLong, C. J., Qin, L., and Cui, Z. (2000). Nuclear localization of enzymatically active green fluorescent protein-CTP:phosphocholine cytidylyltransferase alpha fusion protein is independent of cell cycle conditions and cell types. J. Biol. Chem. *275*, 32325–32330.

Dunne, S. J., Cornell, R. B., Johnson, J. E., Glover, N. R., and Tracey, A. S. (1996). Structure of the membrane binding domain of CTP:phosphocholine cytidylyltransferase. Biochemistry *35*, 11975–11984.

Echevarria, W., Leite, M. F., Guerra, M. T., Zipfel, W. R., and Nathanson, M. H. (2003). Regulation of calcium signals in the nucleus by a nucleoplasmic reticulum. Nat. Cell Biol. *5*, 440–446.

Eriksson, M. *et al.* (2003). Recurrent de novo point mutations in lamin A cause Hutchinson-Gilford progeria syndrome. Nature *423*, 293–298.

Esko, J. D., Wermuth, M. M., and Raetz, C. R. (1981). Thermolabile CDP-choline synthetase in an animal cell mutant defective in lecithin formation. J. Biol. Chem. *256*, 7388–7393.

Fagone, P., Sriburi, R., Ward-Chapman, C., Frank, M., Wang, J., Gunter, C., Brewer, J. W., and Jackowski, S. (2007). Phospholipid biosynthesis program underlying membrane expansion during B-lymphocyte differentiation. J. Biol. Chem. *282*, 7581–7601.

Farsad, K., and De Camilli, P. (2003). Mechanisms of membrane deformation. Curr. Opin. Cell Biol. *15*, 372–381.

Farsad, K., Ringstad, N., Takei, K., Floyd, S. R., Rose, K., and De Camilli, P. (2001). Generation of high curvature membranes mediated by direct endophilin bilayer interactions. J. Cell Biol. *155*, 193–200.

Feldman, D. A., Rounsifer, M. E., and Weinhold, P. A. (1985). The stimulation and binding of CTP:phosphorylcholine cytidylyltransferase by phosphatidylcholine-oleic acid vesicles. Biochim. Biophys. Acta *833*, 429–437.

Ford, M. G., Mills, I. G., Peter, B. J., Vallis, Y., Praefcke, G. J., Evans, P. R., and McMahon, H. T. (2002). Curvature of clathrin-coated pits driven by epsin. Nature *419*, 361–366.

Fricker, M., Hollinshead, M., White, N., and Vaux, D. (1997). Interphase nuclei of many mammalian cell types contain deep, dynamic, tubular membrane-bound invaginations of the nuclear envelope. J. Cell Biol. *136*, 531–544.

Goldman, R. D. *et al.* (2004). Accumulation of mutant lamin A causes progressive changes in nuclear architecture in Hutchinson-Gilford progeria syndrome. Proc. Natl. Acad. Sci. USA *101*, 8963–8968.

Gruenbaum, Y., Margalit, A., Goldman, R. D., Shumaker, D. K., and Wilson, K. L. (2005). The nuclear lamina comes of age. Nat. Rev. Mol. Cell Biol. *6*, 21–31.

Haithcock, E., Dayani, Y., Neufeld, E., Zahand, A. J., Feinstein, N., Mattout, A., Gruenbaum, Y., and Liu, J. (2005). Age-related changes of nuclear architecture in *Caenorhabditis elegans*. Proc. Natl. Acad. Sci. USA *102*, 16690–16695.

Harborth, J., Elbashir, S. M., Bechert, K., Tuschl, T., and Weber, K. (2001). Identification of essential genes in cultured mammalian cells using small interfering RNAs. J. Cell Sci. *114*, 4557–4565.

Helmink, B. A., Braker, J. D., Kent, C., and Friesen, J. A. (2003). Identification of lysine 122 and arginine 196 as important functional residues of rat CTP: phosphocholine cytidylyltransferase alpha. Biochemistry *42*, 5043–5051.

Isaac, C., Pollard, J. W., and Meier, U. T. (2001). Intranuclear endoplasmic reticulum induced by Nopp140 mimics the nucleolar channel system of human endometrium. J. Cell Sci. *114*, 4253–4264.

Izumi, M., Vaughan, O. A., Hutchison, C. J., and Gilbert, D. M. (2000). Head and/or CaaX domain deletions of lamin proteins disrupt preformed lamin A and C but not lamin B structure in mammalian cells. Mol. Biol. Cell *11*, 4323–4337.

Johnson, J. E., Xie, M., Singh, L. M., Edge, R., and Cornell, R. B. (2003a). Both acidic and basic amino acids in an amphitropic enzyme, CTP:phosphocholine cytidylyltransferase, dictate its selectivity for anionic membranes. J. Biol. Chem. *278*, 514–522.

Johnson, N., Krebs, M., Boudreau, R., Giorgi, G., LeGros, M., and Larabell, C. (2003b). Actin-filled nuclear invaginations indicate degree of cell de-differentiation. Differentiation *71*, 414–424.

Lagace, T. A., and Ridgway, N. D. (2005). The rate-limiting enzyme in phosphatidylcholine synthesis regulates proliferation of the nucleoplasmic reticulum. Mol. Biol. Cell *16*, 1120–1130.

Lagace, T. A., Storey, M. K., and Ridgway, N. D. (2000). Regulation of phosphatidylcholine metabolism in Chinese hamster ovary cells by the sterol regulatory element-binding protein (SREBP)/SREBP cleavage-activating protein pathway. J. Biol. Chem. *275*, 14367–14374.

Lammerding, J., Fong, L. G., Ji, J. Y., Reue, K., Stewart, C. L., Young, S. G., and Lee, R. T. (2006). Lamins A and C but not lamin B1 regulate nuclear mechanics. J. Biol. Chem. *281*, 25768–25780.

Lee, E., Marcucci, M., Daniell, L., Pypaert, M., Weisz, O. A., Ochoa, G. C., Farsad, K., Wenk, M. R., and De Camilli, P. (2002). Amphiphysin 2 (Bin1) and T-tubule biogenesis in muscle. Science *297*, 1193–1196.

Lee, M. C., Orci, L., Hamamoto, S., Futai, E., Ravazzola, M., and Schekman, R. (2005). Sar1p N-terminal helix initiates membrane curvature and completes the fission of a COPII vesicle. Cell *122*, 605–617.

Lin, F., and Worman, H. J. (1993). Structural organization of the human gene encoding nuclear lamin A and nuclear lamin C. J. Biol. Chem. *268*, 16321–16326.

Lippincott-Schwartz, J., Snapp, E., and Kenworthy, A. (2001). Studying protein dynamics in living cells. Nat. Rev. Mol. Cell Biol. *2*, 444–456.

Lui, P. P., Lee, C. Y., Tsang, D., and Kong, S. K. (1998). Ca^{2+} is released from the nuclear tubular structure into nucleoplasm in C6 glioma cells after stimulation with phorbol ester. FEBS Lett. *432*, 82–87.

Lykidis, A., Baburina, I., and Jackowski, S. (1999). Distribution of CTP:phosphocholine cytidylyltransferase (CCT) isoforms. Identification of a new CCT-beta splice variant. J. Biol. Chem. *274*, 26992–27001.

Lykidis, A., Murti, K. G., and Jackowski, S. (1998). Cloning and characterization of a second human CTP:phosphocholine cytidylyltransferase. J. Biol. Chem. *273*, 14022–14029.

Marius, P., Guerra, M. T., Nathanson, M. H., Ehrlich, B. E., and Leite, M. F. (2006). Calcium release from ryanodine receptors in the nucleoplasmic reticulum. Cell Calcium *39*, 65–73.

Prufert, K., Vogel, A., and Krohne, G. (2004). The lamin CxxM motif promotes nuclear membrane growth. J. Cell Sci. *117*, 6105–6116.

Prunuske, A. J., and Ullman, K. S. (2006). The nuclear envelope: form and reformation. Curr. Opin. Cell Biol. *18*, 108–116.

Ralle, T., Grund, C., Franke, W. W., and Stick, R. (2004). Intranuclear membrane structure formations by CaaX-containing nuclear proteins. J. Cell Sci. *117*, 6095–6104.

Richieri, G. V., Anel, A., and Kleinfeld, A. M. (1993). Interactions of long-chain fatty acids and albumin: determination of free fatty acid levels using the fluorescent probe ADIFAB. Biochemistry *32*, 7574–7580.

Ridsdale, R., Tseu, I., Wang, J., and Post, M. (2001). CTP:phosphocholine cytidylyltransferase alpha is a cytosolic protein in pulmonary epithelial cells and tissues. J. Biol. Chem. *276*, 49148–49155.

Shackleton, S. *et al.* (2000). LMNA, encoding lamin A/C, is mutated in partial lipodystrophy. Nat. Genet. *24*, 153–156.

Sheetz, M. P., Painter, R. G., and Singer, S. J. (1976). Biological membranes as bilayer couples. III. Compensatory shape changes induced in membranes. J. Cell Biol. *70*, 193–203.

Snapp, E. L., Hegde, R. S., Francolini, M., Lombardo, F., Colombo, S., Pedrazzini, E., Borgese, N., and Lippincott-Schwartz, J. (2003). Formation of stacked ER cisternae by low affinity protein interactions. J. Cell Biol. *163*, 257–269.

Sorensen, V., Brech, A., Khnykin, D., Kolpakova, E., Citores, L., and Olsnes, S. (2004). Deletion mutant of FGFR4 induces onion-like membrane structures in the nucleus. J. Cell Sci. *117*, 1807–1819.

Storey, M. K., Byers, D. M., Cook, H. W., and Ridgway, N. D. (1997). Decreased phosphatidylcholine biosynthesis and abnormal distribution of CTP: phosphocholine cytidylyltransferase in cholesterol auxotrophic Chinese hamster ovary cells. J. Lipid Res. *38*, 711–722.

Taneva, S. G., Patty, P. J., Frisken, B. J., and Cornell, R. B. (2005). CTP: phosphocholine cytidylyltransferase binds anionic phospholipid vesicles in a cross-bridging mode. Biochemistry *44*, 9382–9393.

Veitch, D. P., Gilham, D., and Cornell, R. B. (1998). The role of histidine residues in the HXGH site of CTP:phosphocholine cytidylyltransferase in CTP binding and catalysis. Eur. J. Biochem. *255*, 227–234.

Wang, Y., MacDonald, J. I., and Kent, C. (1993a). Regulation of CTP:phosphocholine cytidylyltransferase in HeLa cells. Effect of oleate on phosphorylation and intracellular localization. J. Biol. Chem. *268*, 5512–5518.

Wang, Y., MacDonald, J. I., and Kent, C. (1995). Identification of the nuclear localization signal of rat liver CTP:phosphocholine cytidylyltransferase. J. Biol. Chem. *270*, 354–360.

Wang, Y., Sweitzer, T. D., Weinhold, P. A., and Kent, C. (1993b). Nuclear localization of soluble CTP:phosphocholine cytidylyltransferase. J. Biol. Chem. *268*, 5899–5904.

Watkins, J. D., and Kent, C. (1992). Immunolocalization of membrane-associated CTP:phosphocholine cytidylyltransferase in phosphatidylcholine-deficient Chinese hamster ovary cells. J. Biol. Chem. *267*, 5686–5692.

Yang, J., Wang, J., Tseu, I., Kuliszewski, M., Lee, W., and Post, M. (1997). Identification of an 11-residue portion of CTP-phosphocholine cytidylyltransferase that is required for enzyme-membrane interactions. Biochem. J. *325*(Pt 1), 29–38.

Yoon, Y., Pitts, K. R., and McNiven, M. A. (2001). Mammalian dynamin-like protein DLP1 tubulates membranes. Mol. Biol. Cell *12*, 2894–2905.

Young, S. G., Meta, M., Yang, S. H., and Fong, L. G. (2006). Prelamin a farnesylation and progeroid syndromes. J. Biol. Chem. *281*, 39741–39745.

Zacharias, D. A., Violin, J. D., Newton, A. C., and Tsien, R. Y. (2002). Partitioning of lipid-modified monomeric GFPs into membrane microdomains of live cells. Science *296*, 913–916.